

## Buried Ni/Cu(001) Interface at the Atomic Scale

H. L. Meyerheim,<sup>1,\*</sup> D. Sander,<sup>1</sup> N. N. Negulyaev,<sup>2</sup> V. S. Stepanyuk,<sup>1</sup> R. Popescu,<sup>1,†</sup> I. Popa,<sup>3</sup> and J. Kirschner<sup>1</sup>

<sup>1</sup>Max-Planck-Institut für Mikrostrukturphysik, Weinberg 2, D-06120 Halle, Germany

<sup>2</sup>Fachbereich Physik, Martin-Luther-Universität, Friedemann-Bach-Platz 6, D-06099 Halle, Germany

<sup>3</sup>ESRF, BP 220, F-38043 Grenoble, France

(Received 7 November 2007; published 9 April 2008)

We present a quantitative surface x-ray analysis of the buried Ni/Cu(001) interface structure after deposition of 3 and 5 monolayers of Ni at room temperature. Interface mixing is found where  $27 \pm 10\%$  of top layer Cu atoms are exchanged by Ni. Atomic scale simulations reveal a kinetic pathway for the Ni/Cu-exchange process and explain the observed limited degree of intermixing. A disperse distribution of Ni within the Cu surface with a preferential Ni-Ni separation of 3–4 nearest neighbor distances is determined.

DOI: [10.1103/PhysRevLett.100.146101](https://doi.org/10.1103/PhysRevLett.100.146101)

PACS numbers: 68.35.Ct, 61.05.C-, 75.70.Ak

Seemingly simple epitaxial systems often exhibit striking physical properties in the nanometer thickness range. A wealth of structural and magnetic peculiarities has been identified for ferromagnetic monolayers on Cu(001) [1]. Prototypes are the growth of fcc Fe with both ferromagnetic and antiferromagnetic order [1,2], and the inverse spin reorientation transition of Ni from an easy magnetization direction in-plane to out-of-plane with *increasing* film thickness [3,4].

One major factor which plays a key role for the peculiar properties of monolayers is the lattice misfit between film and substrate. The misfit-induced 3-dimensional strain renders the cubic film material in a tetragonally distorted lattice, which is the origin of a significant contribution to the magnetic anisotropy [3,5,6]. Recent theoretical works on Ni/Cu(001) have clearly identified that in addition to the structural distortion of the film, also *both* interfaces, substrate-film and film-vacuum, influence the magnetic anisotropy considerably [4,7,8].

The outer film-vacuum interface has been subject to numerous investigations which convincingly demonstrated that adsorption and structural relaxation at the film-vacuum interface offer a handle to influence the magnetic anisotropy of the film [4,9]. However, the buried interface is covered by several atomic layers of Ni, and therefore its detailed structural and chemical analysis is demanding, and corresponding studies are scarce [10]. A most important issue in this respect is exchange between film and substrate atoms. It has been reported to modify not only the magnetic anisotropy [11], but also the transport properties through the interface drastically [12].

Previous analyses of the interface structure were unable to provide an unambiguous picture of the Ni/Cu-interface structure. Scanning tunneling microscopy did either not detect interface mixing [13] or was not able to attribute different gray levels to definite alloy compositions [14]. The analysis of low energy electron diffraction experiments [15–17] suffers from the very similar scattering amplitudes of Ni and Cu and from the limited penetration

depth of the electrons, seriously complicating the analysis of the buried interface. Consequently, conflicting structure models have been proposed: e.g., in contrast to Müller *et al.* [15] and Platow *et al.* [17], Kim *et al.* [16] propose a Cu-cap layer on top of the Ni film.

In our combined surface x-ray diffraction (SXRD) and molecular dynamics (MD) study of the Ni/Cu(001) interface we find sizeable intermixing between Ni and Cu to occur for growth at 300 K, where up to 30% of the interface atoms are exchanged. Intermixing is confined to the layers directly adjacent to the interface. The Ni atoms are non-regularly dispersed within the Cu matrix at a preferential separation of more than 2 nearest-neighbor distances. Expelled Cu atoms, however, form compact Cu islands within the growing Ni film.

The experiments were carried out at the beamline ID03 of the European Synchrotron Radiation Facility in Grenoble (France) using an UHV diffractometer. The Cu(001) crystal was prepared by standard methods and Ni films of 3 and 5 ML thickness were deposited *in situ* by evaporation from a Ni rod heated by electron bombardment. The deposition rate ( $F \approx 0.16$  ML/min) was calibrated with high precision from the measurement of reflection intensity oscillations at the (1 0 0.1) position along the (10 $\ell$ ) crystal truncation rod (CTR) [18,19]. Here, we use the primitive setting of the surface unit cell.

Integrated x-ray reflection intensities were collected under grazing incidence of the primary x-ray beam ( $\lambda = 0.72$  Å) by rotating the sample about its surface normal [18]. The average standard deviation of in total 182 symmetry equivalent reflection intensities along the (10 $\ell$ ), (11 $\ell$ ), (20 $\ell$ ) and (21 $\ell$ ) CTRs is as low as 3.9%, comparable in quality only with experiments in bulk crystallography.

The structure factor amplitudes  $|F|$  were derived from the integrated intensities by correcting the data for geometric factors [20]. Symbols in Fig. 1 represent the  $|F|$ 's for the 3 ML (lower curves) and the 5 ML samples (upper curves), respectively. Solid lines represent the best fits to the experimental data. The fit quality is expressed by the

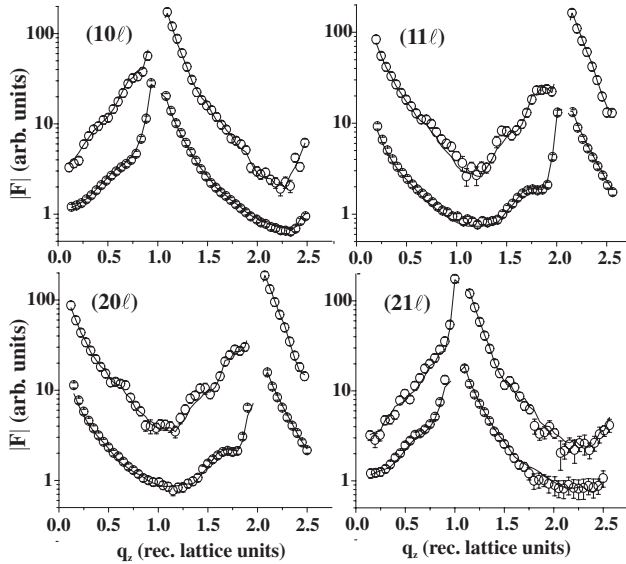


FIG. 1. Measured (symbols) and calculated (lines) structure factor amplitudes along several crystal truncation rods for 3 ML (lower curves) and 5 ML (upper curves) Ni on Cu(001). Curves are shifted vertically for clarity.

unweighted residuum ( $R_u$ ) and by the goodness of fit parameter (GOF) [18]. We find GOF values of 0.94 and 1.06 and residua of 0.058 and 0.053 for the 3 and 5 ML samples, respectively, which can be considered excellent. In the following we discuss the structure model on the basis of the 3 ML sample, whose interface structure is representative for the 5 ML sample also.

Figure 2 shows a side view of the structure model. Bright and dark spheres represent Ni and Cu atoms, respectively. Because of the high symmetry (4 mm) of the atomic sites within the unit cell, only the  $z$  position and the Debye parameter ( $B$ ), representing thermal disorder [21], need to be refined for each layer. Including an overall scale factor, we obtain 15–20 parameters, which—in view of the number of data points (182)—ensures a sufficient overdetermination of the refinement problem.

The most important result is that  $27 \pm 10\%$  of the top layer Cu atoms (layer 5) are exchanged by Ni atoms. Substituted Cu atoms are incorporated into the first Ni

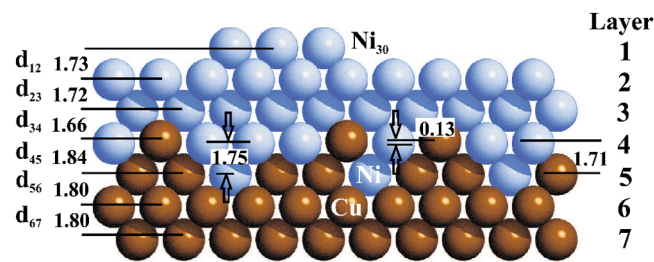


FIG. 2 (color online). Structure model for 3 ML Ni/Cu(001). Bright and dark balls represent Ni and Cu atoms, respectively. Distances are indicated in Å units. Layers are numbered from 1 (top) to 7 (bottom) on the right.

layer (layer 4). In addition, the  $z$  positions of the Ni and Cu atoms and of the first substrate layer were refined. Numbers in Fig. 2 indicate the interlayer spacings ( $d_{ij}$ ), with an error bar of  $\pm 0.03$  Å.

The fit quality is improved by allowing the Ni atoms in layer 4 to relax inward by  $\Delta z = 0.13$  Å leading to a vertical Ni-Cu spacing across the intermixed interface of 1.71 Å, while the Cu-Cu spacing and the Ni-Ni-spacing are 1.84 and 1.75 Å, respectively.

Figure 3 shows a contour plot of the GOF parameter versus  $\Delta z$  ( $x$  axis) and the degree of intermixing given by  $\theta_{\text{Ni}}$  ( $y$  axis), the amount of Ni in the top Cu layer and vice versa. All other parameters were also varied in order to include the correlations between the parameters.

A GOF minimum of 0.94 is found for  $\Delta z = 0.13$  Å and  $\theta_{\text{Ni}} = 0.27$  (0.28 for the 5 ML sample). From the variation of GOF on the parameters we estimate error bars of about  $\pm 0.10$  for  $\theta_{\text{Ni}}$  and about  $\pm 0.03$  Å for  $\Delta z$ . For instance, excluding any intermixing and rumpling ( $\theta_{\text{Ni}} = 0$ ,  $\Delta z = 0$ ) leads to a GOF value of about 1 (lower left in Fig. 3), i.e., 6% worse than the best fit.

The experimental observations are complemented by *ab initio* calculations and MD simulations. First, we consider the interaction between two Ni atoms by calculating the interaction energies between nearest neighbor sites (NN)[22] in the bulk and at the surface layer. We have used the *ab initio* VASP ultrasoft pseudopotential package within the generalized gradient approximation [23]. The interaction energies are defined as the total energy difference between the dimer complex and two isolated impurities. Calculations are carried out in a fully relaxed geometry. For bulk NN sites the interaction between two Ni atoms is attractive ( $-30$  meV) while it is repulsive

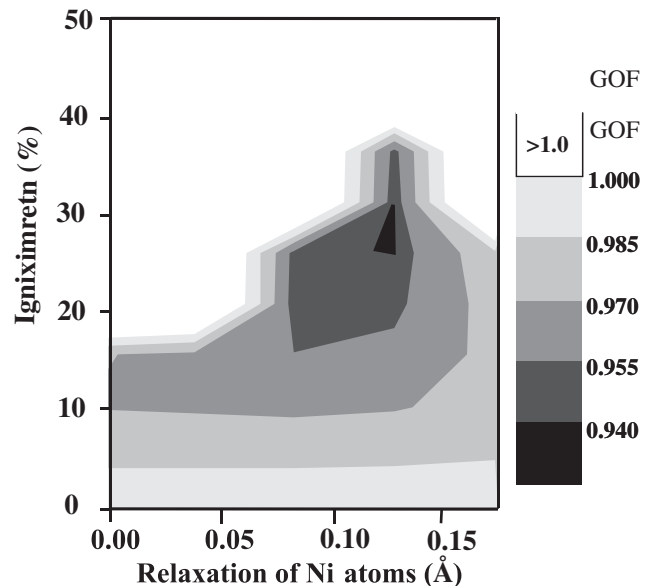


FIG. 3. Contour plot of GOF versus degree of intermixing in percent of a ML and layer rumpling expressed by the inward relaxation of Ni atoms in layer 4.

(+ 10 meV) in the topmost surface layer [24]. Here, positive values indicate a tendency for the formation of a dispersed alloy, whereas negative ones reveal a tendency for phase separation.

These results can be explained by the tight-binding model of Meunier *et al.* [25]. For the Ag/Cu system it has been shown that due to the broken bonds the interaction energy between impurities at the surface is less attractive than that in the bulk in a fully relaxed geometry. This model even predicts a change of the sign of the interaction energy at a surface. Such a reversal has been reported for the Au/Ni [26] and the Ag/Cu [27] system. The driving force for the surface-confined mixing can be attributed to broken bonds at the surface and to atomic size mismatch [28]. Tersoff has shown that the strain will cause two impurities to repel in the surface [28]. However, in marked contrast to these systems, the interaction energies in Ni/Cu as well as the strain relaxations are rather small. Therefore the structure of the Ni/Cu interface could be strongly determined by *kinetics* rather than by energetics.

To gain detailed insight into the growth process in the case of Ni/Cu at the atomic scale we have carried out MD simulations using the interatomic potentials for Ni and Cu formulated in the second moment approximation of the tight-binding approach [29]. The density functional theory calculations (Korringa-Kohn-Rostocker Green's function method [30]) are used to create an *ab initio* data pool for the fitting of potential parameters [31,32].

Our simulations reveal that for given experimental conditions the interface evolution can be subdivided into three stages. The *first stage* (coverage of Ni  $\leq 0.3$  ML) is characterized by strong exchange of deposited Ni with the Cu atoms of the topmost layer. As a rule, the incorporation of a Ni atom takes place (i) in the vicinity of the region, where the atom lands, and (ii) at  $>2\text{NN}$  position [22] with respect to already embedded Ni (the incorporation into the NN or 2NN positions is suppressed). It leads to the growth of an array of embedded Ni atoms with 3NN or 4NN separation [22] (Fig. 4). At the end of the first stage, the fraction of embedded Ni atoms is equal to 0.24. Substituted Cu atoms and nonembedded Ni atoms coalesce in the first layer into nanoislands with a nucleation density of about  $0.04$  islands/nm<sup>2</sup>.

During the *second stage* ( $\sim 0.3$ – $1.0$  ML) the concentration of Ni atoms within the topmost Cu substrate layer increases only by 0.01. Any Ni embedding during this stage would involve incorporation at NN or 2NN separation with respect to already embedded Ni atoms, but such atomic processes are suppressed as will be discussed below in detail. Deposited Ni atoms stay predominantly in the first layer and coalesce with existing nanoislands. During the *third stage* ( $1.0$ – $3.0$  ML) subsequent formation of the second and third Ni overlayer by layer-by-layer growth takes place. Both layers consist of Ni atoms. Figure 4(a) schematically illustrates the composition of the topmost Cu layer at the buried Cu-Ni interface after deposition of 3.0 ML of Ni. Figure 4(b) specifies the number of em-

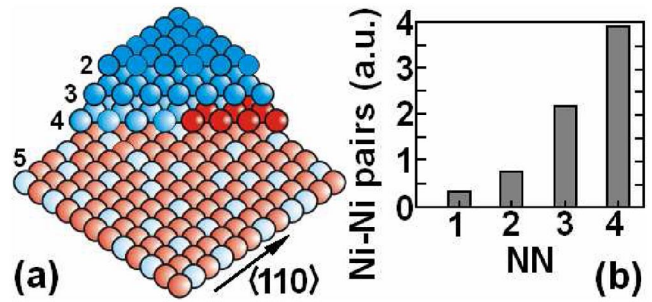


FIG. 4 (color online). (a) Calculated atomic composition of the topmost  $3 \times 3$  nm<sup>2</sup> Cu layer after deposition of 3.0 ML of Ni. Dark and light balls represent Cu and Ni atoms, respectively. Layers are numbered as in Fig. 2. The majority of the film has been removed to expose the topmost Cu surface layer 5. (b) Number of embedded Ni pairs vs Ni-Ni separation. The majority of Ni atoms is separated by  $d > 2\text{NN}$ .

bedded Ni-Ni pairs vs Ni-Ni separation. The total fraction of embedded Ni is 0.25, in excellent agreement with the SXRD data ( $0.27 \pm 0.10$ ).

In the following we explain why the formation of embedded Ni-Ni pairs with NN or 2NN separation is suppressed. First, as we have already discussed, energetically such pairs are unfavorable. Additionally, the characteristic time scale  $t_c$  for the growth process is determined by the ratio  $D/F$ , where  $D$  is the characteristic dose and  $F$  is the flux. Embedding of deposited atoms takes place only in the submonolayer regime; therefore  $D \sim 0.1$  ML. Setting  $F$  to  $0.16$  ML/min we obtain that  $t_c \sim 0.6$  min. On the other hand, the average time  $t_a$  of a thermally activated atomic process is estimated as  $t_a = v_0^{-1} \exp(E_b/k_B T)$ , where  $E_b$  is the activation barrier,  $T$  is the temperature,  $k_B$  is the Boltzmann constant, and  $v_0$  is a prefactor. The examined atomic process of intermixing is operative only if  $t_a < t_c$ . Setting  $v_0 = 10^{12}$  Hz and  $T = 300$  K, we obtain that atomic events with barriers  $E_b > E_{cr} = 0.75$  eV are suppressed in the studied system under the experimental conditions.

The MD calculations with the interatomic potentials [31] indicate that the energy barrier  $E_b$  for the incorporation of a Ni atom into the clean Cu(001) surface is equal to 0.65 eV. This value is less than  $E_{cr}$ ; therefore, this process is operative. The energy barrier  $E_b$  for the embedding of Ni into the Cu surface, where Ni atoms are already incorporated, depends on the distance of the deposited atom to the embedded Ni atom. For incorporation into the NN or 2NN sites [22] with respect to the embedded Ni,  $E_b$  is equal to 0.83 and 0.77 eV, respectively. In the first case  $E_b$  is too large and almost no Ni-Ni pairs at NN distances are formed. In the second case,  $E_b$  is close to  $E_{cr}$ ; therefore, embedding into the 2NN position is operative, although with a low probability. Incorporation at the 3NN and the 4NN sites is characterized by  $E_b = 0.65$  eV, i.e., such processes take place. On the other hand,  $E_b$  for the incorporation of Ni into the second Cu layer below the interface



is equal to 2.4 eV, i.e., much larger than  $E_{cr}$ , which explains why interface mixing is confined to the top Cu layer only.

While embedding of Ni atoms into the first Cu layer is an energetically favorable process, the finite flux ( $F$ ) sets the limit for the degree of intermixing. It should be emphasized that the intermixing process is of kinetic rather than of energetic origin. We suggest that tailoring of the interface structure can be achieved by variation of  $F$  and  $T$ , where a high flux at low temperature favors atomically sharp interfaces with little intermixing. For example, decreasing the temperature to 200 K suppresses the interface intermixing. The intermixing can be also reduced by increasing the flux.

Most remarkably, our results indicate that the atomic exchange at the interface is (i) limited to the interface region, and (ii) is limited to 30% of exchanged atoms at the interface. This differs drastically from Ni-Cu bulk alloys, where an intermixing of the two species in all proportions is found [33].

Our results also provide an explanation for the markedly different behavior of intermixing reported for the Fe/Cu(001) interface, where Fe forms embedded clusters in the Cu surface [34], whereas embedded Ni atoms stay dispersed. Our calculation reveals that the energy of the attractive interaction between Fe atoms in the surface layer is rather strong (more than 0.2 eV); therefore, the cluster formation is energetically favorable. The barrier for exchange of the Fe adatom with a Cu atom next to an already embedded Fe atom equals 0.72 eV, and therefore this collective exchange mechanism is operative. The situation is reversed for Ni, where the collective exchange process has a larger barrier (0.83 eV) as compared to the diffusion away from an embedded Ni atom (0.70 eV); therefore embedded Ni atoms do not agglomerate.

In conclusion, we have provided a quantitative SXRD analysis of the atomic exchange at the buried Cu/Ni interface, which is in excellent agreement with atomic scale simulations. We reveal that intermixing between Ni and Cu is caused by kinetic processes, which limit the degree of Ni incorporation to roughly 0.3 ML. The intermixing is spatially confined to two atomic layers adjacent to the interface, where also considerable rumpling is observed near Ni atoms within the Cu matrix. In view of the delicate dependence of the physical properties of this prototype epitaxial system on the detailed structure [4] these results have profound implications for future state of the art experimental studies and electronic structure calculations.

\*hmeyerhm@mpi-halle.mpg.de

†Labor f. Elektronenmikroskopie, Universität Karlsruhe, D-76128 Karlsruhe.

[1] M. Wuttig and X. Liu, *Ultrathin Metal Films*, Springer Tracts in Modern Physics (Springer, New York, 2004), Vol. 206.

- [2] J. Thomassen *et al.*, Phys. Rev. Lett. **69**, 3831 (1992).  
 [3] B. Schulz and K. Baberschke, Phys. Rev. B **50**, 13467 (1994).  
 [4] J. Hong *et al.*, Phys. Rev. Lett. **92**, 147202 (2004).  
 [5] D. Sander, Rep. Prog. Phys. **62**, 809 (1999).  
 [6] M. Ciria *et al.*, Phys. Rev. B **70**, 054431 (2004).  
 [7] C. Uiberacker *et al.*, Phys. Rev. Lett. **82**, 1289 (1999).  
 [8] F. Máca *et al.*, Czech. J. Phys. **53**, 33 (2003); J. Magn. Magn. Mater. **272**, 1194 (2004).  
 [9] D. Sander *et al.*, Phys. Rev. Lett. **93**, 247203 (2004).  
 [10] E. Holmstrom *et al.*, Phys. Rev. Lett. **97**, 266106 (2006).  
 [11] C. Liu *et al.*, Phys. Rev. Lett. **60**, 2422 (1988).  
 [12] C. Sommers and P. Weinberger, Phys. Rev. B **72**, 054431 (2005).  
 [13] J. Shen *et al.*, Phys. Rev. B **52**, 8454 (1995).  
 [14] J. Lindner *et al.*, Phys. Rev. B **62**, 10431 (2000).  
 [15] S. Müller *et al.*, Surf. Sci. **364**, 235 (1996).  
 [16] S. H. Kim *et al.*, Phys. Rev. B **55**, 7904 (1997).  
 [17] W. Platow *et al.*, Phys. Rev. B **59**, 12641 (1999).  
 [18] I. K. Robinson and D. J. Tweet, Rep. Prog. Phys. **55**, 599 (1992).  
 [19] I. K. Robinson Phys. Rev. B **33**, 3830 (1986).  
 [20] E. Vlieg, J. Appl. Crystallogr. **30**, 532 (1997).  
 [21] M. J. Buerger, *Contemporary Crystallography* (McGraw-Hill, New York, 1970).  
 [22] Lateral separations between neighbors (ng) are defined as follows (distances in Å): NN = 2.56 (nearest ng), 2NN = 3.62 (next nearest ng), 3NN = 5.12 (next next nearest ng) and 4NN = 5.72 (next next next nearest ng).  
 [23] G. Kresse and J. Hafner, Phys. Rev. B **48**, 13115 (1993); G. Kresse and J. Furthmüller, Phys. Rev. B **54**, 11169 (1996); G. Kresse and D. Joubert, Phys. Rev. B **59**, 1758 (1999).  
 [24] The interaction for the 2NN in the topmost surface layer is very weak being also repulsive (+ 2 meV).  
 [25] I. Meunier *et al.*, Surf. Sci. **441**, 225 (1999).  
 [26] J. Jacobsen *et al.*, Phys. Rev. Lett. **75**, 489 (1995).  
 [27] P. T. Sprunger *et al.*, Phys. Rev. B **54**, 8163 (1996).  
 [28] J. Tersoff, Phys. Rev. Lett. **74**, 434 (1995).  
 [29] V. Rosato *et al.*, Philos. Mag. A **59**, 321 (1989); F. Cleri and V. Rosato, Phys. Rev. B **48**, 22 (1993).  
 [30] K. Wildberger *et al.*, Phys. Rev. Lett. **75**, 509 (1995); V. S. Stepanyuk *et al.*, Phys. Rev. B **53**, 2121 (1996).  
 [31] The potentials are used in the form of Ref. [29]. The parameters are the following for Cu-Cu:  $A^1 = 0.0$  eV,  $A^0 = 0.0854$  eV,  $\xi = 1.2243$  eV,  $p = 10.939$ ,  $q = 2.2799$ ,  $r_0 = 2.5563$  Å; for Ni-Cu:  $A^1 = -1.2613$  eV,  $A^0 = -0.0242$  eV,  $\xi = 1.0245$  eV,  $p = 7.5119$ ,  $q = 3.8115$ ,  $r_0 = 2.5312$  Å; for Ni-Ni:  $A^1 = 0.0$  eV,  $A^0 = 0.0409$  eV,  $\xi = 1.2526$  eV,  $p = 13.1458$ ,  $q = 1.9442$ ,  $r_0 = 2.6171$  Å. Formation of Ni clusters in the Cu bulk has been observed in simulations at finite temperatures using our potentials.  
 [32] N. A. Levanov *et al.*, Phys. Rev. B **61**, 2230 (2000).  
 [33] *Binary Alloy Phase Diagrams*, edited by T. B. Massalski, H. Okamoto, P. R. Subramanian, and L. Kacprzak (American Society for Metals, Metals Park, OH, 1990), 2nd ed., Vol. 2.  
 [34] D. D. Chambliss and K. E. Johnson, Phys. Rev. B **50**, 5012 (1994); R. Longo *et al.*, Phys. Rev. B **69**, 073406 (2004).